Multipath trapping dynamics of nanoparticles towards an integrated waveguide with a high index contrast

Citation: Tian, Hao et al. "Multipath Trapping Dynamics of Nanoparticles Towards an Integrated Waveguide with a High Index Contrast." Proceedings of SPIE, Microfluidics, BioMEMS, and Medical Microsystems XV, Janaury 28 - February 2 2017, San Francisco, California, USA, edited by Bonnie L. Gray and Holger Becker, SPIE, February 2017 © 2017 SPIE

As Published: http://dx.doi.org/10.1117/12.2251590

Publisher: SPIE

Persistent URL: http://hdl.handle.net/1721.1/112292

Version: Final published version: final published article, as it appeared in a journal, conference proceedings, or other formally published context

PROCEEDINGS OF SPIE

SPIEDigitalLibrary.org/conference-proceedings-of-spie

Multipath trapping dynamics of nanoparticles towards an integrated waveguide with a high index contrast

Hao Tian, Lionel C. Kimerling, Jurgen Michel, Guifang Li, Lin Zhang

SPIE.

Multipath Trapping Dynamics of Nanoparticles towards an Integrated Waveguide with a High Index Contrast

Hao Tian[a,b,c], Lionel C. Kimerling[c], Jurgen Michel[c], Guifang Li[a,b,d], and Lin Zhang[a,b,c]

[a]Key Laboratory of Opto-electronic Information Technical Science of Ministry of Education, School of Precision Instruments and Opto-electronics Engineering, Tianjin University, Tianjin 300072, China

[b]Key Laboratory of Integrated Opto-electronic Technologies and Devices in Tianjin, School of Precision Instruments and Opto-electronics Engineering, Tianjin University, Tianjin 300072, China

[c]Microphotonics Center, Department of Material Science and Engineering, Massachusetts Institute of Technology, Cambridge, MA 02139, USA

[d]College of Optics and Photonics, CREOL and FPCE, University of Central Florida. 4000 Central Florida Blvd. Orlando, FL 32816. USA

ABSTRACT

Optical trapping and manipulation of nanoparticles in integrated photonics devices have recently received increasingly more attention and greatly facilitated the advances in lab-on-chip technologies. In this work, by solving motion equation numerically, we study the trapping dynamics of a nanoparticle near a high-index-contrast slot waveguide, under the influence of water flow perpendicular to the waveguide. It is shown that a nanoparticle can go along different paths before it gets trapped, strongly depending on its initial position relative to the integrated waveguide. Due to localized optical field enhancement on waveguide sidewalls, there are multiple trapping positions, with a critical area where particle trapping and transport are unstable. As the water velocity increases, the effective trapping range shrinks, but with a rate that is smaller than the increasing of water velocity. Finally, the trapping range is shown to decrease for smaller slot width that is below 100 nm, even though smaller slot width generates stronger local optical force.

Keywords: Optical trapping, optofluidics, dynamic model, slot waveguide, nanoparticle

1. INTRODUCTION

Optical trapping of micro- and nano-particles has attracted much interest since the first demonstration of it by Ashkin *et al*. in 1970.[1] It has found wide applications in biophotonics, chemical sensing/monitoring, and microscopy. Later, the optical manipulation has been achieved in integrated photonics scenario,[2] which greatly extends the flexibility and dimensions of optical trapping and can be integrated easily with optofluidics devices, facilitating the capability of lab-on-chip technologies to a large extent.[3] Many integrated photonic structures have been proposed and utilized to realize particle transport, trapping, sorting and storage, such as waveguide,[4–7] resonator,[8–11] photonic crystal,[12–15] and plasmonic devices.[16,17] Among these, nanophotonic devices with high index contrast provide high optical field confinement and enhancement, and thus strong optical gradient force.[18,19] On the other hand, the high index contrast structure usually exhibits unique modal power distribution which forms complicated optical trapping potential wells. Nevertheless, the optical trapping design and analysis is performed in static case where the particle is assumed to be already trapped and the optical force is calculated accordingly.[19,20] Then, the optical force and trapping stiffness are often used to evaluate device performance. However, there has been little reported on nanoparticle trapping dynamics,[21,22] which tracks

Further author information: (Send correspondence to Jurgen Michel and Lin Zhang)
Jurgen Michel: E-mail: jmichel@mit.edu
Lin Zhang: E-mail: lin_zhang@tju.edu.cn

Microfluidics, BioMEMS, and Medical Microsystems XV, edited by Bonnie L. Gray, Holger Becker, Proc. of SPIE Vol. 10061, 100610P · © 2017 SPIE · CCC code: 1605-7422/17/$18 · doi: 10.1117/12.2251590

trajectories of particles in the optical field and flowing fluid. This would give us more insight into the optical manipulation and comprehensive performance of the device in practical applications.

In this paper, a dynamic model is established to illustrate the trajectory of a nanoparticle moving near a slot waveguide with a high refractive index contrast, in the case with the flowing water perpendicular to the waveguide. The optical field enhancement at the waveguide sidewalls produces trapping potentials that are comparable with that formed in the slot. The particle from different initial positions may go along different paths and be trapped by either the slot or waveguide sidewalls, determined by the competition between the forces produced at the slot, sidewalls and by the water flow. It is found that there exists a critical area where the particle transport is unstable, resulting in dramatically different trapping locations. The influence of the water velocity is examined, showing how water drag force competes with optical trapping potentials. The trapping range for different water velocities and slot widths is identified, which comprehensively illustrates how the nano-structured waveguides perform in real operation.

2. METHOD

The waveguide is shown in Fig. 1(a), which consists of a nano-scale slot in the middle of the Si waveguide on SiO_2 substrate and is placed in a microfluidic channel. The waveguide height and width are 220 nm and 500 nm, respectively, and the slot is 50 nm wide. A 50-nm-diameter polystyrene particle is carried by water flowing perpendicular to the waveguide and is attracted to the waveguide due to optical force.[19] The refractive index of the particle is 1.59.[2] Continuous-wave laser light at 1550 nm wavelength is launched into the waveguide.

A particle moves in the channel under gravity $\mathbf{F_g}$, buoyant force $\mathbf{F_b}$, optical force $\mathbf{F_{opt}}$, water drag force $\mathbf{F_{drag}}$ and Brownian force. Basically, its movement is governed by Newton's law, as shown in Eq. (1). By solving it numerically, one can simulate particle dynamics. To simplify the problem, we treat the particle as a mass point and do not consider its rotation. Since we aim at high-sensitivity detection, the concentration of particle is low, and thus particles' diffusion effect can be ignored. The electric double layer (EDL) effect near waveguide surfaces[23,24] can also be diminished by adjusting ionic strength of the fluid.[19,20]

$$m\ddot{\mathbf{s}} = \mathbf{F_g} + \mathbf{F_b} + \mathbf{F_{opt}} + \mathbf{F_{drag}} \tag{1}$$

Gravitational force is $\mathbf{F_g} = -mg_0\hat{\mathbf{y}}$, and buoyant force $\mathbf{F_b} = \rho_m \mathrm{v} g_0 \hat{\mathbf{y}}$ where ρ_m is the density of water which is 1000 kg/m^3, and v is the volume of particle. In order to calculate optical force, we need to know optical mode distribution. It is computed using a standard mode solver and is shown in Fig. 1(b). The slot waveguide has strong field confinement and thus light intensity in the slot due to the electric field discontinuity of the TE mode at material interfaces.[18,25] Similarly, there is also field enhancement on the waveguide sidewalls, with trapping potential wells formed, which can be strong enough to compete with that at the waveguide center.

The optical force of a particle is calculated based on Maxwell stress tensor[6] as given in Eq. (2).

$$\langle \mathbf{T_M} \rangle = \mathbf{D}\mathbf{E}^* + \mathbf{H}\mathbf{B}^* - \frac{1}{2}(\mathbf{D}\cdot\mathbf{E}^* + \mathbf{H}\cdot\mathbf{B}^*)\mathbf{I} \tag{2}$$

where $\mathbf{I}$ is isotropic tensor. We integrate the time-averaged Maxwell stress tensor over a sphere surface (with a radius that is larger than particle radius by 2 nm), which encloses the particle,[20] in order to avoid the possible problem introduced by the discontinuity of optical field at the particle surface (Eq. (3)).[6]

$$\mathbf{F_{EM}} = \oint_{\mathbf{s}} (\langle \mathbf{T_M} \rangle \cdot \mathbf{n})\, \mathrm{d}S \tag{3}$$

We obtain the distribution of optical force at the waveguide top surface (e.g. 30 nm above) by changing the position of the particle, as shown in Fig. 1(d). It is noted that F_y is maximum at the waveguide center, while it forms two small peaks at the waveguide sidewalls which can also trap particles. One can determine whether particle is trapped at the center or the sidewalls by analyzing particle dynamics.

Then, we obtain the distribution of water flow. In general, water flow in microfluidics is assumed to be incompressible Newtonian fluid, so it is described by Navier-Stokes equation:[21]

$$\rho_m \left(\frac{\partial \mathbf{u}}{\partial t} + \mathbf{u}\cdot\nabla\mathbf{u} \right) = -\nabla p + \mu\nabla^2\mathbf{u} \tag{4}$$

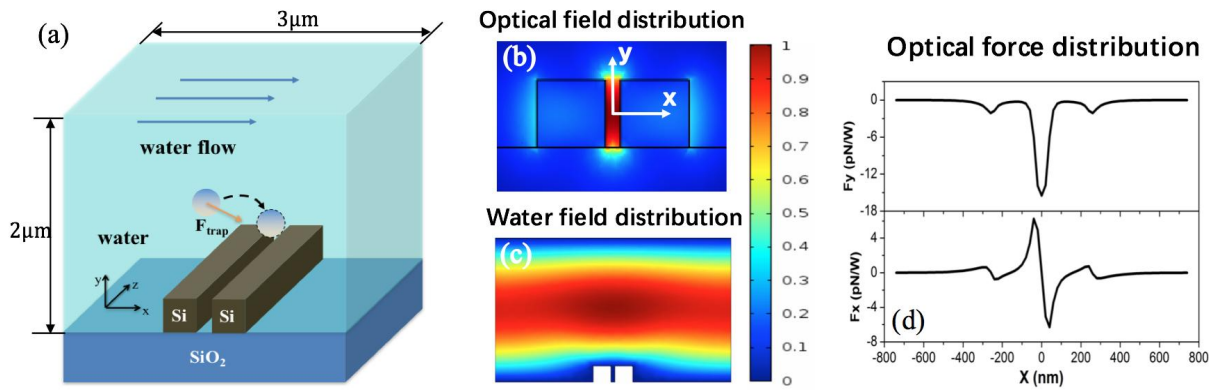

Figure 1. (a) Schematic of slot waveguide (500×220 nm^2) with a 50-nm slot in a microfluidic channel. Water flows perpendicular to the waveguide with average water velocity, 0.25 cm/s. A 50-nm particle is carried by the water and attracted to the waveguide due to optical force. Distributions of (b) optical field and (c) water field (water velocity u_x) of the slot waveguide. The intensity is normalized by the maximum value in both (b) and (c). The origin and definition of coordinate is shown in (b). Quasi-TE mode is excited by the light at 1550 nm wavelength. (d) Distribution of optical force $\mathbf{F_{opt}}$ at 30 nm above the waveguide surface.

where $\mathbf{u}$ is the velocity of water flow, p is the pressure, and μ is viscosity of water which is 1×10^{-3} Pa·s. In microfluidics, due to the very low Reynold number, water flow is mainly a laminar flow.[20–22] The water velocity field can be simulated numerically using COMSOL Multiphysics. 'No-slip' boundary condition is used at the waveguide and channel surfaces,[21,22] and we set the average water velocity to be u_a as a variable in our model. Since the particle is very small, we assume the existence of particle does not affect the distribution of water velocity, which is calculated without particle in it, as shown in Fig. 1(c). In this work, water flows perpendicular to the waveguide, with the main component of the water velocity being u_x. We see from Fig. 1(c) that the velocity's main component is maximum at the channel center, and it is near zero at waveguide surface.

Since the radius of particle r_p is 25 nm, the Reynold number of the particle, $(2r_p\rho_m|\mathbf{u}-\mathbf{v_p}|/\mu)$, is around 10^{-5}.[21] In this range, we can calculate the water drag force using the Stokes law:[21,22,26]

$$\mathbf{F_{drag}} = 6\pi\mu r_p(\mathbf{u}-\mathbf{v_p}) \tag{5}$$

Water drag force is proportional to the relative velocity between particle and water. However, if a particle is very small relative to the mean free path of water molecules, the water fluid can no longer be considered as a continuum.[27] To determine this, we can calculate the Knudson number, K_n, of the particle, which is the ratio of mean free path and particle diameter.[27] In our case, K_n is 0.006 which is around the critical point. In this range, the no-slip condition at the particle boundary in deriving Stokes equation is no longer true. Thus, we should use the Cunningham correction factor, C_c, which is $1/(1+2.52K_n) = 0.9851$, to multiply the drag force coefficient, to take the non-continuum effect of water into account.[27]

3. DYNAMIC ANALYSIS

Since the water velocity is perpendicular to the waveguide (flowing in the X direction), it generates drag force that tends to pull the trapped particle away from the waveguide. In this case, the magnitude of water velocity shows a great influence on particle trapping, which can be analyzed using the dynamic model. At first, the water velocity is fixed to 0.25 cm/s, we find out different trajectories of 50-nm particlesas shown in Fig. 2(a), which are released from different initial X positions but the same height (100 nm above the waveguide top surface). For X_0 = -300 nm, outside the waveguide (two waveguide sidewalls are located at X = -250 and 250 nm), the particle overcomes the trapping potential at the waveguide edge under the drag force of the water flow and continues to move to the waveguide center, and finally is trapped in the slot. A particle with X_0 = -200 nm is carried by water and naturally trapped in the slot, while it is a little beyond expectation that a particle with X_0 = 50 nm moves against the water flow and is still trapped at the center. For particles with X_0 = 100 nm and 200 nm, they can escape from the trapping potential of the slot and are finally trapped at the waveguide sidewall, X =

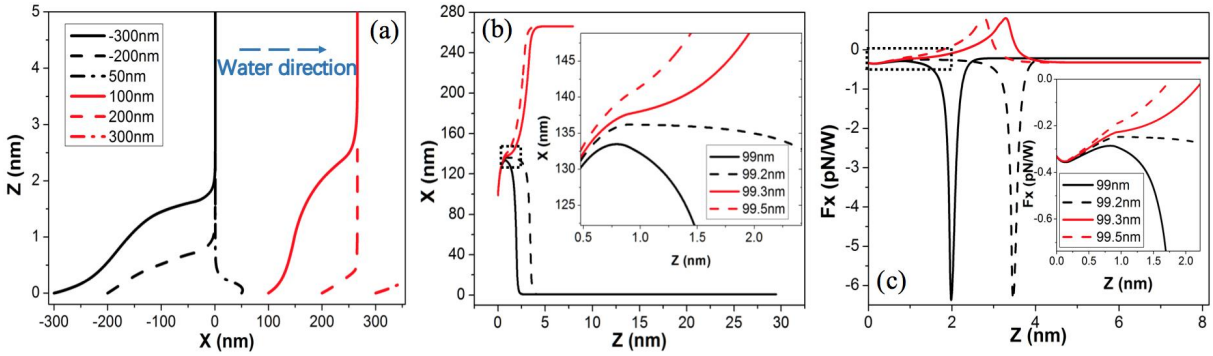

Figure 2. (a) Trajectories of particles for different initial X positions in the X-Z plane. Change of the particle's (b) position and (c) F_x for particles with the initial X position around the critical point. Insets show the zoom-in of curves around the critical area. Initial heights of them are all 100 nm above the waveguide top surface, and water velocity is 0.25 cm/s which is perpendicular to the waveguide.

266 nm. In contrast, since the trapping well near the sidewall is so weak that the particle with X_0 = 300 nm moves with the water flow without being attracted by the sidewall. We note that all the particles slightly move in the Z direction simultaneously, because of the optical scattering force.

Between X_0 = 50 and 100 nm, the particle changes gradually from the center trapping to the sidewall trapping. In Fig. 2(b) is the movement of the particle around the critical area where optical trapping becomes unstable. Initially, the particles follow similar trajectory and move towards the sidewall, carried by water flow. However, when the particle falls on the waveguide, depending on the sign of the total force (optical force plus water drag force), the particles may exhibit dramatically different trajectories even with only a slightly changed initial position by 0.1 nm (see black dashed and red solid lines). From the dynamic model, we can get more details in the force evolution in Fig. 2(c). At the beginning, the optical force is negative, pointing to the waveguide center. However, since the height of the particle initially is high, the water velocity is also higher. Thus, particles move along with the water firstly. As the particle goes down and moves closer to the sidewall, the magnitude of the optical force decreases gradually, and at the same time, the water drag force is reducing due to the smaller water velocity. When the particle moves near X = 135 nm, F_x is around -0.25 pN, which can balance the water drag force. If the particle is closer to the sidewall and the magnitude of optical force is smaller than 0.25 pN (red lines), the particle is trapped on the waveguide sidewall, because the water drag force is stronger, and the optical force gradually changes the direction. For the black lines, the F_x overcomes water flow and the magnitude of it increases dramatically as the particle is attracted by the slot. Finally, the optical force is stabilized around -0.25 pN again, which together with water drag force generates zero net force.

Interestingly, there exists a state (e.g. X_0 = 99.2 nm) where the forces in the X direction from the slot, sidewall, and water balance with each other. Because of this, the particle has little movement in the X direction over a certain distance, while moving along the waveguide. However, this state is unstable, and the particle is finally trapped either by the slot or the sidewall if any deviation exists. Therefore, the movement direction and trapping location of a particle is determined by the competition among the two optical forces produced by the optical fields on the slot and sidewall and the force given by the water field. The dynamic model reveals the instability of particle transport around the critical area, which would become uncertain due to Brownian motion.

With the same initial position, the particle can also be trapped at different places if water velocity varies, as shown in Fig. 3. For X_0 = -300 nm, when the water velocity is as small as 0.1 cm/s, the particle gradually approaches the trapping potential well around the waveguide sidewall, X = -250 nm. Differently, at water velocity of 0.2 cm/s, the particle flies over the trapping site first and then is attracted back while falling down, as shown in Fig. 3(a). The dynamic model reveals that the optical force on the sidewall increases as the particle falls down and is stronger than the water drag force. If the water velocity increases further to 0.5 or 1.2 cm/s, the particle can overcome the potential well at the sidewall and be trapped at the waveguide center. We note that, if the water velocity is so large (e.g. 1.4 cm/s) that the particle cannot be trapped at the waveguide center, it will no longer be trapped at the other sidewall-induced potential at X = 250 nm. This is because the optical force

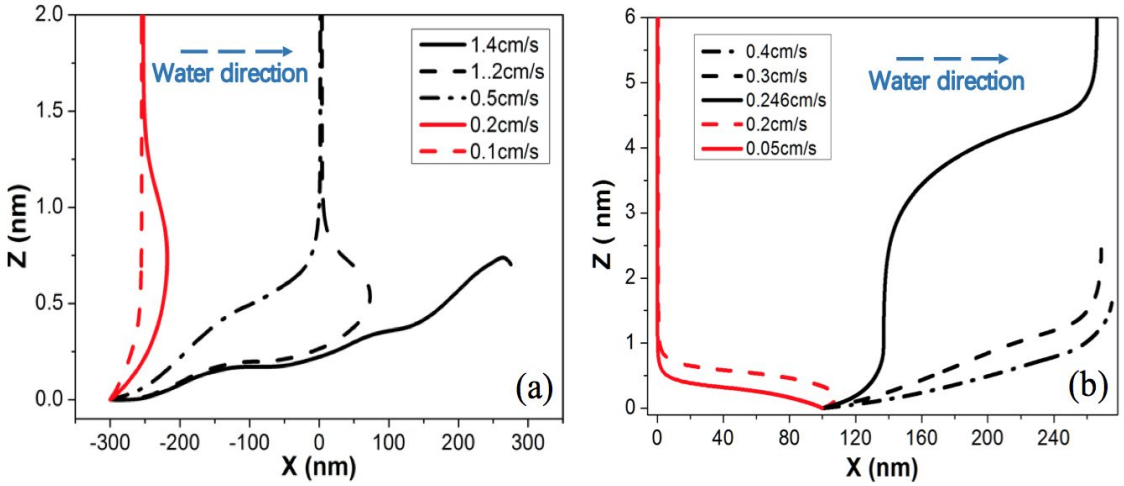

Figure 3. Trajectories of particles in the X-Z plane with initial position (a) X_0 = -300 nm and (b) X_0 = 100 nm under different water velocities. Initial Y position is 100 nm above the waveguide top surface.

at the center is much larger than that on the sidewall, and once the water velocity is large enough to overcome the slot-induced optical force, the water drag force exerted to the particle will be stronger than the force on the other sidewall for sure. Thus, the particle finally flows away.

Then, we conduct another study, i.e., with X_0 = 100 nm. When the water velocity is small enough (red lines in Fig. 3(b)), the particle is attracted towards the waveguide center. As the water velocity increases to 0.3 cm/s, the particle can escape potential well at the center and be trapped at the sidewall. As the water velocity is even larger (0.4 cm/s), the particle can no longer be trapped by the waveguide. Note that the water velocity at 0.246 cm/s is a critical point differentiating between the center trapping and the sidewall trapping, as shown in Fig. 3(b). Similarly, the particle reaches the state that the net force in X direction is nearly zero, but it finally escapes this unstable state and is trapped at the sidewall.

It is indispensable to consider the trapping range of a device in practice, within which the particle can be trapped by the waveguide. Using the dynamic model, we find the trapping range for a slot waveguide with different water velocities in Fig. 4(a). Particles between two red lines are trapped at the waveguide center, while particles between two adjacent red and black lines are trapped at two sidewalls. As the water velocity increases, the trapping range shrinks gradually. At a low water velocity (0.01 and 0.2 cm/s), the particle can be trapped at either the two sidewalls or the center of the waveguide. However, in the case of 0.2 cm/s, particle trapping requires a much smaller initial Y_0. At a water velocity of 0.4 cm/s, the particle cannot be trapped at the right sidewall (X = 250 nm), since the drag force is larger than the maximum force on that sidewall. However, the particle can still be trapped at the left side, because the local water velocity is reduced by the left sidewall. As the water velocity increases further, e.g. 0.8 cm/s, the trapping range becomes even smaller (the particle has to be close enough to the waveguide in the vertical direction), and the particle can only be trapped at the waveguide center.

Fig. 4(b) clearly shows how the trapping range changes with the water velocity. We only plot curves for the center trapping. It is important to note that, from 0.1 to 1.6 cm/s, the water velocity is doubled every time, but the interval between adjacent two lines is nearly equal. This means that the decreasing rate of the trapping range is smaller than the increasing speed of the water velocity. We attribute this to the fact that the waveguide is at the bottom of the microfluidic channel where the water velocity is relatively small due to the no-slip condition. The influence of doubling the water velocity is thus small too. Even when the average water velocity is increased to 3 cm/s, the particle can still be trapped to the slot as long as its height is <100 nm.

The dynamic model also enables us to examine the influence of the slot width on the trapping range. One usually uses the trapping stability, stiffness or the maximum force to measure the trapping ability of a device.[3,20] In order to obtain a large force, we need a small slot width to have a large field enhancement factor inside the

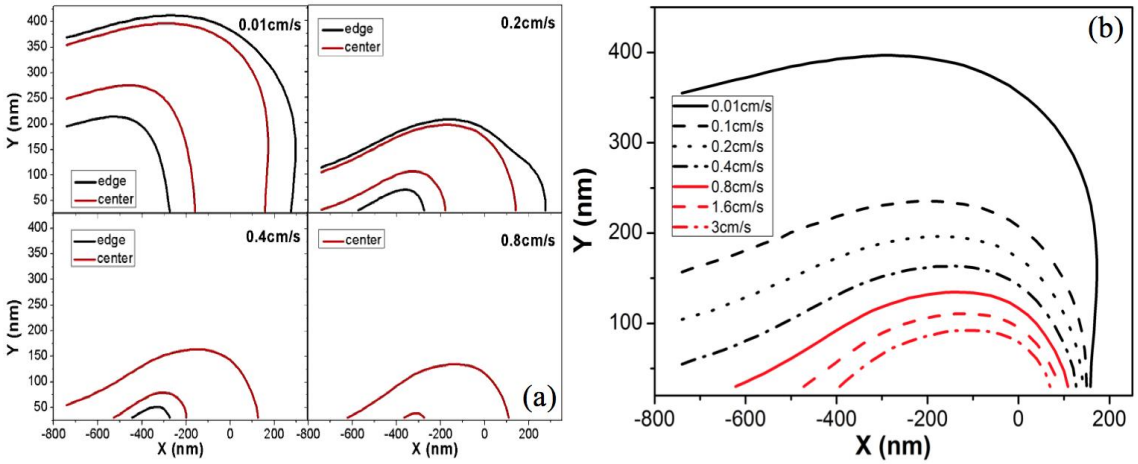

Figure 4. (a) Trapping range of the slot waveguide under different water velocities. Particles between two red lines are trapped at the waveguide center, while particles between two adjacent red and black lines are trapped at two sidewalls. (b) The center trapping range (the upper red line in (a)) shrinks with an increased water velocity.

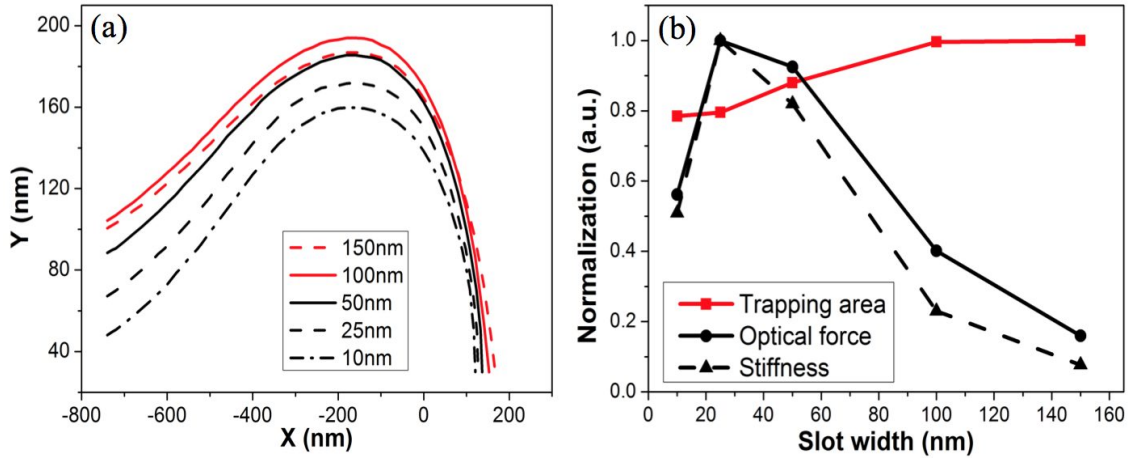

Figure 5. (a) Center trapping range for different slot widths, at a water velocity of 0.25 cm/s. (b) Normalized trapping area, optical force, and stiffness for different slot width. They are normalized to their corresponding maximum values. The stiffness is obtained by calculating the slope of the optical force around the center

slot. However, using a small slot means that the optical force is localized to a small area, which reduces the trapping range. In other words, this is a trade-off between the optical trapping stability and the trapping range. Similar issues occur in other kinds of structures, such as the photonic-crystal-based optical traps.[13,28] In Fig. 5, the slot width is changed from 10 to 150 nm, and we see that the 100-nm slot has the biggest trapping range for the center trapping. As the slot width decreases, the trapping range shrinks. On the other hand, as shown in Fig. 5(b) where all the parameters are normalized by their maximum values, the optical force and stiffness of the 25-nm slot is the largest, and the influence of the slot width on the optical force and stiffness is bigger than the trapping area. Thus, one can choose a suitable slot width (like 50-nm slot in this case) to improve the trapping performance of a slot waveguide in terms of a large optical force and an optimal trapping area.

4. CONCLUSION

In this work, to understand the dynamics of a nanoparticle under the influence of the forces from the optical field of the nanophotonic waveguide and the water field, a dynamic model is established by numerically solving the motion equation. Due to the high-index contrast of the slot waveguide, there is strongly localized optical field enhancement on waveguide sidewalls, which have the potential to compete with the slot and trap nanoparticles.

The water flow is perpendicular to the waveguide and generates drag force that may overcome the trapping potential. Depending on its initial position, the nanoparticle can follow different paths before it becomes trapped, and shows multiple trapping sites. There exists a critical area between slot and sidewalls trapping, where the particle trapping and transport become unstable. The influence of water velocity is also analyzed and found to significantly affect the final trapping position of the particle. The effective trapping range gradually decreases with the increasing of the water velocity, but at a smaller rate. Finally, the trapping range starts to decrease when the slot width reduces to below 100 nm. Although a smaller slot width possesses a larger local optical force and stiffness, which guarantees stable particle trapping, one may have to use a relatively large slot width to increase trapping range.

REFERENCES

[1] Ashkin, A., "Acceleration and trapping of particles by radiation pressure," *Physical review letters* **24**(4), 156 (1970).

[2] Kawata, S. and Tani, T., "Optically driven mie particles in an evanescent field along a channeled waveguide," *Optics letters* **21**(21), 1768–1770 (1996).

[3] Erickson, D., Serey, X., Chen, Y.-F., and Mandal, S., "Nanomanipulation using near field photonics," *Lab on a Chip* **11**(6), 995–1009 (2011).

[4] Ng, L., Zervas, M., Wilkinson, J., and Luff, B., "Manipulation of colloidal gold nanoparticles in the evanescent field of a channel waveguide," *Applied Physics Letters* **76**(15), 1993–1995 (2000).

[5] Gaugiran, S., Gétin, S., Fedeli, J., Colas, G., Fuchs, A., Chatelain, F., and Dérouard, J., "Optical manipulation of microparticles and cells on silicon nitride waveguides," *Optics Express* **13**(18), 6956–6963 (2005).

[6] Schmidt, B. S., Yang, A. H., Erickson, D., and Lipson, M., "Optofluidic trapping and transport on solid core waveguides within a microfluidic device," *Optics Express* **15**(22), 14322–14334 (2007).

[7] Yang, A. H., Moore, S. D., Schmidt, B. S., Klug, M., Lipson, M., and Erickson, D., "Optical manipulation of nanoparticles and biomolecules in sub-wavelength slot waveguides," *Nature* **457**(7225), 71–75 (2009).

[8] Arnold, S., Keng, D., Shopova, S., Holler, S., Zurawsky, W., and Vollmer, F., "Whispering gallery mode carousel–a photonic mechanism for enhanced nanoparticle detection in biosensing," *Optics Express* **17**(8), 6230–6238 (2009).

[9] Cai, H. and Poon, A. W., "Optical manipulation of microparticles using whispering-gallery modes in a silicon nitride microdisk resonator," *Optics letters* **36**(21), 4257–4259 (2011).

[10] Yang, A. H. and Erickson, D., "Optofluidic ring resonator switch for optical particle transport," *Lab on a Chip* **10**(6), 769–774 (2010).

[11] Lin, S., Schonbrun, E., and Crozier, K., "Optical manipulation with planar silicon microring resonators," *Nano letters* **10**(7), 2408–2411 (2010).

[12] Serey, X., Mandal, S., and Erickson, D., "Comparison of silicon photonic crystal resonator designs for optical trapping of nanomaterials," *Nanotechnology* **21**(30), 305202 (2010).

[13] Lin, S., Hu, J., Kimerling, L., and Crozier, K., "Design of nanoslotted photonic crystal waveguide cavities for single nanoparticle trapping and detection," *Optics letters* **34**(21), 3451–3453 (2009).

[14] Mandal, S., Serey, X., and Erickson, D., "Nanomanipulation using silicon photonic crystal resonators," *Nano letters* **10**(1), 99–104 (2009).

[15] Barth, M. and Benson, O., "Manipulation of dielectric particles using photonic crystal cavities," *Applied physics letters* **89**(25), 253114 (2006).

[16] Cao, T. and Cryan, M. J., "Modeling of optical trapping using double negative index fishnet metamaterials," *Progress In Electromagnetics Research* **129**, 33–49 (2012).

[17] Lin, P.-T., Chu, H.-Y., Lu, T.-W., and Lee, P.-T., "Trapping particles using waveguide-coupled gold bowtie plasmonic tweezers," *Lab on a Chip* **14**(24), 4647–4652 (2014).

[18] Almeida, V. R., Xu, Q., Barrios, C. A., and Lipson, M., "Guiding and confining light in void nanostructure," *Optics letters* **29**(11), 1209–1211 (2004).

[19] Yang, A. H., Lerdsuchatawanich, T., and Erickson, D., "Forces and transport velocities for a particle in a slot waveguide," *Nano letters* **9**(3), 1182–1188 (2009).

[20] Yang, A. H. and Erickson, D., "Stability analysis of optofluidic transport on solid-core waveguiding structures," *Nanotechnology* **19**(4), 045704 (2008).

[21] Heiniger, A. T., Miller, B. L., and Fauchet, P. M., "Optical and fluidic design for guaranteed trapping and detection of particles in a silicon microfluidic and photonic crystal system," in [*Proc. SPIE*], **7888**, 78880L (2011).

[22] Heiniger, A. T., Miller, B. L., and Fauchet, P. M., "Numerical study of sensitivity enhancement in a photonic crystal microcavity biosensor due to optical forces," *Optics Express* **23**(19), 25072–25083 (2015).

[23] Greberg, H. and Kjellander, R., "Charge inversion in electric double layers and effects of different sizes for counterions and coions," *The Journal of chemical physics* **108**(7), 2940–2953 (1998).

[24] Hansen, J.-P. and Lowen, H., "Effective interactions between electric double-layers," *arXiv preprint cond-mat/0002295* (2000).

[25] Majumder, S. and Chakraborty, R., "Semianalytical method to study silicon slot waveguides for optical sensing application," *Optical Engineering* **52**(10), 107102–107102 (2013).

[26] Richardson, J. F., Harker, J. H., and Backhurst, J. R., [*Chemical Engineering*], vol. 2, Butterworth-Heinemann, Oxford, 5 ed. (2002).

[27] Haghshenas-Jaryani, M., Black, B., Ghaffari, S., Drake, J., Bowling, A., and Mohanty, S., "Dynamics of microscopic objects in optical tweezers: experimental determination of underdamped regime and numerical simulation using multiscale analysis," *Nonlinear Dynamics* **76**(2), 1013–1030 (2014).

[28] Ma, J., Martínez, L. J., and Povinelli, M. L., "Optical trapping via guided resonance modes in a slot-suzuki-phase photonic crystal lattice," *Optics express* **20**(6), 6816–6824 (2012).